Comparative Investigation of Yield and Quality of Carbon Nanotubes by Catalytic Conversion of Recycled Polypropylene and Polyethylene Plastics Over Fe-Co-Mo/CaCO$_3$ Based on Chemical Vapour Deposition

Matthew Adah Onu[1*], Olusola Olaitan Ayeleru[1], Bilainu Oboirien[2], Peter Apata Olubambi[1]

[1] Centre for Nanoengineering and Advanced Material, University of Johannesburg, Doornfontein Campus, 2028, Johannesburg, South Africa

[2] Department of Chemical Engineering, University of Johannesburg, Doornfontein Campus, 2028, Johannesburg, South Africa

* Corresponding author's email: meetchiefonu@gmail.com

ABSTRACT

Polypropylene (PP) and polyethylene (PE) plastic waste is accumulating in the environment and the oceans at an alarming rate. The current management methods, mostly landfilling and incineration, are becoming unsustainable. In this study, thermal catalytic conversion of waste PP and PE polymers into carbon nanotubes (CNTs) using a trimetallic catalyst prepared from the nitrate salts of iron, cobalt, and molybdenum supported with calcium carbonate was reported. The yield and quality of multi-walled carbon nanotubes (MWCNTs) produced were investigated. The findings showed a high graphitic value for the CNTs obtained from PP and PE, as corroborated by the d-spacing of XRD. The I_D/I_G ratio of CNTs synthesized from PP and PE as carbon sources were 0.6724 and 0.9028, respectively, which showed that CNT produced from PP has more ordered graphite. The functional groups present in the produced CNTs were determined via FITR analysis. The BET and Langmuir surface areas were found to be (6.834 and 70.468 m^2/g) and (6.733 and 70.347 m^2/g) for CNTs obtained from PP and PE respectively. The d-spacing was computed as 0.3425 nm and 0.3442 nm for CNTs made from PP and PE. These fall within the graphite's d-spacing at 0.335 nm. The TGA showed high percentage purity of 94.71 and 94.40% for the products obtained from PP and PE, respectively. The findings showed that recycled PP and PE could be good alternative carbon sources for CNT production.

Keywords: Carbon nanotubes, waste plastic, circular economy, waste valorization, chemical vapour decomposition.

INTRODUCTION

The discovery of synthetic plastic materials several years ago has brought about several technological innovations in human endeavours [1]. In almost every aspect of human society, plastics have been used in electronics, packaging industries, household utensils, automobile parts, roofing, and ceiling materials [1, 2]. The proliferation of polymer materials over the years has also brought about environmental and health hazards due to their non-biodegradability, making them a primary global concern [3]. Recycled plastics comprise polypropylene (PP) and polyethylene (PE), which are often referred to as commodity plastics due to their large volume of production and usage [4]. These plastic materials are commonly used daily, accumulating plastic wastes (PWs) within the municipal solid waste (MSW) stream. However, the current methods of plastic waste (PW), which are purely by landfilling and incineration, are unsustainable, and there are insufficient land spaces within the metropolis for the construction of new disposal facilities [1, 5]. Hence, transforming plastic wastes into new materials of great value like carbon nanotubes (CNTs) is a promising route for environmental sustainability [6, 7]. CNTs have become

much-researched material recently [8], owing to their distinctive and captivating characteristics [9], such as high tensile strength, mechanical strength, electrical toughness, high surface-to-volume ratios for use in different fields like electronics, sensors, biomedical, energy storage, reinforced composites, water treatment and many more [3, 10-13]. The use of CNTs is still limited due to their high cost [14], hence, the use of recycled plastics as cheap feedstocks to produce CNTs would provide a sustainable way of PWs management [15]. Basically, CNTs are classified based on the number of walls formed, which could be single-walls (SWs) or multiple walls (MWs) [16, 17]. Several approaches have been exploited in the fabrication of CNTs, which include plasma-assisted deposition, arc discharge, microwave-assisted synthesis, laser ablation, pyrolysis and chemical vapor deposition (CVD) [18-22]. Amongst these methods, CVD is the most commonly used method due to its relatively low-cost technology for large-scale production and allows for effective manipulation of synthesis parameters for high-quality CNTs formation [11, 23, 24], The production of CNTs by CVD is mostly carried out in the presence of catalysts of transition metals origin supported on different substrate [11]. These transition metals can be used as mono-metallic, bi-metallic, trimetallic, or poly-metallic for CNTs synthesis [10, 12, 25]. Catalysts composition is a crucial component in achieving the required nanoparticle size, morphology, and quality [10]. In their study, Abdulkareem, et al. [11] reported that the yield and quality of CNTs depend primarily on the carbon precursor and appropriate synthesis parameters [11]. The carbon feedstock mainly used for CNTs production via the CVD method has been reported to be ethylene, acetylene, methane, carbon monoxide (CO) and alcohol [11, 12, 25]. A more environmental and economical carbon source such as PWs to produce value-added materials such as CNTs is of great importance to researchers.

Recycled PP and PE have been reported to be potential hydrocarbon feedstock owing to their high carbon value and they are commonly available in large quantities [26, 27]. Wang et al. [28], in their study, reported the catalytic pyrolysis of recycled PP in a two-stage fixed reactor over a nickel-based catalyst and achieved 94% filamentous carbon yield [29]. In their work, Li et al. , produced CNTs of diameter 20–30 nm and a few micrometers long by catalytic pyrolysis of PE over Fe-Ni bi-metallic catalyst [3]. Modekwe,

et al. [10] synthesized CNTs from waste PP over $NiMo/TiO_3$ using the CVD technique and obtained a 44% yield [10]. It has been reported that the more of the combination of metallic catalysts, the better the resultant effect on the yield and quality of CNTs produced [12]. Although the use of the combination of metallic catalysts on a suitable substrate would enhance the yield and quality of CNTs. The trimetallic and quaternary metallic catalysts reported in the literature utilized petroleum hydrocarbon gases as carbon feedstock. However, the use of trimetallic catalyst using waste plastic remains a route that has not received much attention. In this study, a trimetallic catalyst has been developed by wet impregnation from the nitrate salts of iron (Fe), cobalt (Co), and molybdenum (Mo) supported on $CaCO_3$ for the catalytic decomposition of recycled PP and PE in CVD to produce CNTs. Recent studies have shown that iron catalyst has excellent catalytic activity on hydrocarbon dissolution, leading to high CNT yield but low graphitization. Using Co results in high graphitization of CNTs but with low yield, and Mo improves the dispersion and enhances the catalyst's performance [12, 25]. It is hypothesized that combining these metals would improve the quality and yield of CNTs synthesized using recycled PP and PE plastics. To the extent that we are aware, no work has reported the production of CNTs from recycled PP and PE over the trimetallic catalyst and compared its quality and yield. This work described the wet impregnation method of $Fe-Co-Mo/CaCO_3$ catalyst preparation and application with recycled PP and PE as feed for synthesizing CNTs.

MATERIALS AND METHODS

Materials

Recycled PP and PE were obtained from the University of Johannesburg (UJ) Doornfontein Campus (DFC) recycling facility. Samples were cleaned and left to dry at ambient temperature. The color coding on the samples was removed using acetone and shredded using scissors (2–3 mm). Iron nitrate nonahydrate [$(Fe(NO_3)_2.9H_2O)$, $\geq 98.10\%$ trace metals basis], Cobalt nitrate hexahydrate $(Co(NO_3)_2.6H_2O)$, $\geq 98\%$, Ammonium molybdate tetrahydrate $((NH_4)6Mo_7O_{24}.4H_2O)$, $\geq 98.98\%$, Calcium trioxocarbonate $(CaCO_3)$, 99% and deionized water were employed in the

development of the catalyst. All chemicals were used as supplied by Sigma-Aldrich Chemicals Company South Africa.

Preparation of Fe-Co-Mo/CaCO₃ catalysts

For the preparation of Fe-Co-Mo/CaCO₃ catalysts, the wet impregnation method, a procedure similar to that reported by Rather [30], was adapted with slight modification. The catalysts weight composition of 5Fe:3Co:2Mo: 40CaCO₃ was employed. A higher Fe ratio was chosen based on the fact that Fe has higher carbon solubility and will enhance the large quantity of carbon precipitation, which is a vital step for improved MW-CNTs development [31]. In the preparation of the catalyst, 14.46 g of $Fe(NO_3)_2.9H_2O$, 7.19 g of $Co(NO_3)_2.6H_2O$, and 0.80 g $(NH_4)6Mo_7O_{24}.4H_2O$ were mixed in 50 mL deionized water in a 100 mL beaker and the blend was vigorously agitated via magnetic stirrer for 30 min to ensure uniformity, 16.0 g of $CaCO_3$ support was introduced into the solution, allowed to age, continuously agitated for 3 h and subsequently desiccated at 120 °C in an oven. The prepared catalyst was pulverized and calcined at 700 °C for 3 h and kept for application.

Production of CNTs

A CVD setup comprising a horizontal furnace and a quartz tube reactor of 110 cm by 50 mm dimensions was used for the synthesis of CNTs. A quartz boat holding 0.1 g of catalyst evenly spread was positioned in the center of the reactor, and the power source was switched on. The heating commenced at a ramped temperature of 10 °C/min until the target temperature of 750 °C was achieved. The catalyst was left for 30 min to undergo a complete reduction in the presence of 5 vol% of Hydrogen and 95 vol% Argon gases at a flow rate of 90 sccm. A second ceramic boat with 1.0 g of recycled PP was positioned in the moderate temperature region of the reactor next to the catalyst-bearing quartz boat, and the reaction was left to proceed continuously for 30 min and the furnace power source was subsequently turned off. The furnace was left to cool overnight in a nitrogen environment. To ensure the accuracy of the findings, the experiment repeated in triplicate. The process was repeated using PE as feed subsequently. The yield of the deposited carbon with respect to the feed and catalyst was determined utilizing equations (1) and (2) respectively:

$$Y_f (\%) = \frac{M2 - M1}{M3} \times 100 \qquad (1)$$

$$Y_c (\%) = \frac{M2 - M1}{M1} \times 100 \qquad (2)$$

where: Y_f and Y_c are yield based on feed and catalyst, respectively;
M_1 is the mass of the catalyst used;
M_2 is the mass of the catalyst and deposited CNTs;
M_3 is the recycled PP/PE mass used as a carbon source.

Characterization of catalyst (Fe–Co–Mo/CaCO₃) and CNTs

X-ray diffraction (XRD) was utilized to determine the mineralogical composition of the prepared catalyst and MWCNTs. This investigation was done via a Bruker AXS D8 Advance utilizing Cu-K radiation and a scan velocity current of 40 mA operating at an acceleration voltage of 40 kV. Fourier Transmission Infrared (FTIR) spectroscopy analysis was performed using Thermo Scientific FTIR device with wave numbers range of 4000 to 500 cm⁻¹ in absorption mode, using KBr to prepare the samples into a disc-like pattern. Employing a Micromeritics ASAP 2460 (Micromeritics, Atlanta, GA, USA) and particle analyzer for surface area at -196 °C for nitrogen physisorption study, the textural characteristics of the produced CNTs were identified. The sample was degassed by a Micromeritics flow Prep 060 sample degas system for 3 h at 300 °C, 0.25 g of CNT was degassed under vacuum before being subjected to the analysis. The specific surface area, pore size and pore volume of the CNTs were determined by adsorption-desorption isotherm process. Scanning electron microscopy (SEM) was performed with JSM7900F high-resolution scanning electron microscope (HR-SEM) (United Kingdom). The samples were crushed and sputter-coated with a thin layer of carbon and adhered to the two-sided carbon tape, which was fastened to a glass slide and then inserted into the SEM compartment for examination. The Energy-dispersive X-ray (EDX) attached to the SEM was utilized to determine the elemental compositions of the samples. Transmission electron microscopy (TEM) was done using a JEOL JEM-2100 at a voltage of 200 kV. A small amount of the sample powder was mixed with 100% ethanol

and sonicated for 10 min. The prepared sample was dropped onto a copper grid, and the solvent was allowed to dry before taking TEM images. Images of the selected area electron diffraction structure were also captured. Perkin Elma STA 4000 was used to perform thermal profiles on the catalysts and MWCNTs. The thermal behaviour of the CNTs were examined from 50 to 1000 °C at a ramped temperature of 10 °C/min using 11 mg of the sample in an air environment at a flow rate of 20 mL/min. The WiTec focus innovations Raman spectroscopy (Germany) with a Raman shift from 800–3500 cm^{-1} at 532.105 nm excitation wavelength and a diode Nd: YAG laser operating at an ambient temperature condition was used to establish the graphitic quality of the synthesized CNTs. Samples were exposed for 10 seconds on a 10-mW laser.

RESULTS AND DISCUSSION

Characterization of prepared catalyst

X-ray diffraction (XRD) evaluation

XRD study was employed to ascertain the crystallinity and the crystalline phases of the catalyst sample, as shown in Figure 1. The XRD spectra of the Fe-Co-Mo/CaCO$_3$ catalyst revealed the diffraction points at 2θ values of 33°, 37°, 43° and 61°, which correspond to the reflection crystal planes of (110), (111), (200) and (000) respectively [11]. The measured XRD pattern matches various phases. The diffraction peaks at 2θ consists of CaO (01-078-0649) at 2θ value of 32°, 37°, 54°, 64°, 80°, and 89°, Ca$_2$Fe$_2$O$_5$ (00-049-1555) at 2θ value of 29°, 33°, 47°, 52°, 59°, 64°, and 67°, CaMoO$_4$ (04-013-6758) at 2θ value of 19°, 31°, 32°, 34°, 37°, 45°, 49°, 54°, 67°, 76.11° and 80.0°, Ca$_2$Co$_2$O$_5$ (04-016-9652) at 2θ value of 18°, 23°, 45°, 47°, 48.0°, 51°, 54.0°, and 59.5° and CaCO$_3$ (01-072-1937) 2θ value of 36°, 40°, 43°, 56°, 86° and 87°. The presence of Fe, Co, and Mo in the produced catalysts has been established by the XRD spectra and the results were consistent with published data [11, 32].

Scanning electron microscopy (SEM) and energy dispersive X-ray (EDX)

The morphology and elemental composition of the catalyst were examined, and the findings are depicted in Figure 2. The HR-SEM image (Figure 2a) showed a homogenously well dispersed and clustered metallic grains on the surface of the support material. The produced catalyst's porous surface was visible in the micrograph, which would facilitate the transport of the vapour generated from the feedstock onto the catalyst's active site during the synthesis of CNTs. To determine the catalyst's elemental composition, the elemental dispersive X-ray (EDX) technique was used. The EDX was obtained in the binding energy range of 0–10 KeV, as presented in Figure 2b. The EDX spectra showed that Fe, Co, Mo, Ca, O, and C were present in various percentage compositions.
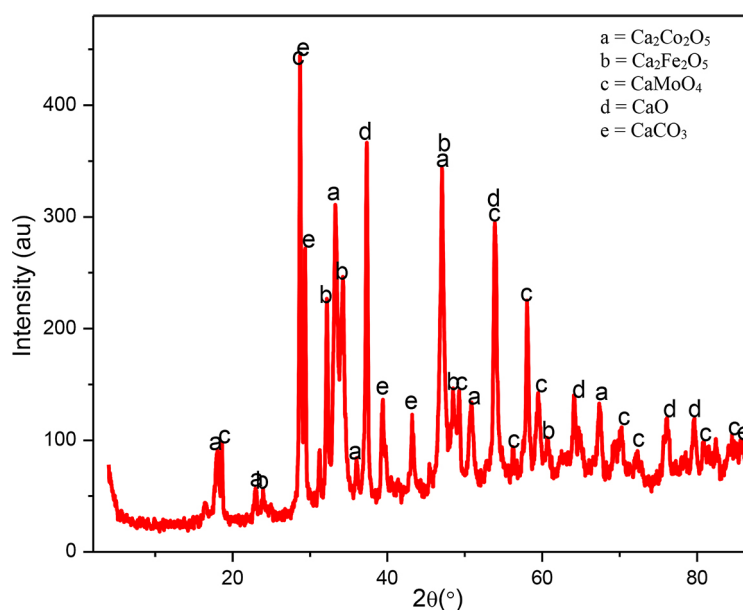

Fig. 1. XRD spectra of Fe-Co-Mo/CaCO$_3$ catalyst applied in the synthesize CNTs
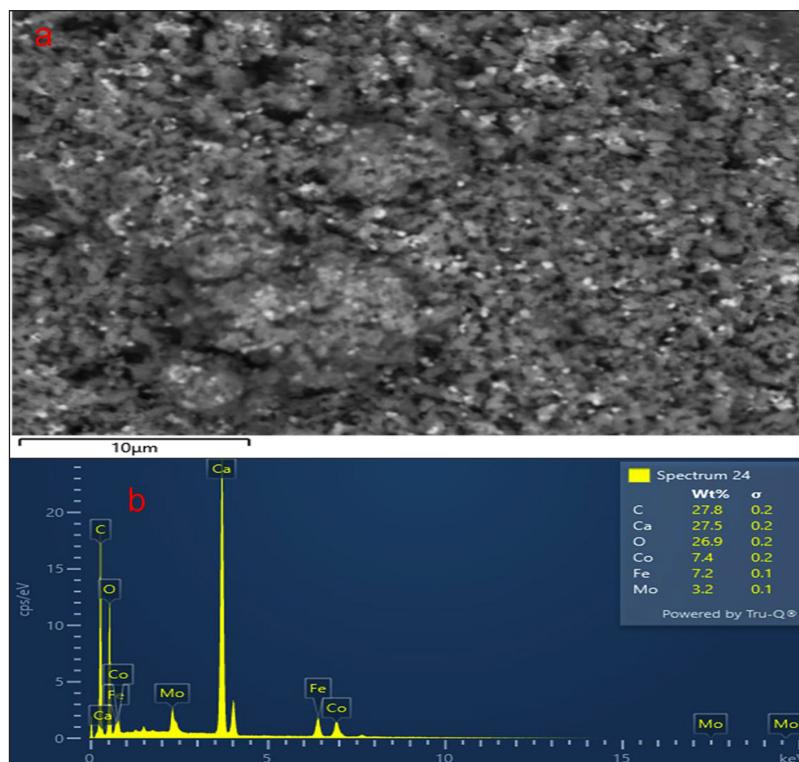
Fig. 2. (a) SEM morphology and (b) EDX spectra of Fe-Co-Mo/CaCO₃ catalyst

The atomic proportion of Fe, Co, Mo, Ca, O and C are shown in Figure 2b. Based on the EDX result, oxygen (O) has a higher percentage value of 38.0%. The increase in the oxygen percentage could result from the decomposition of the metal salts to metallic oxides during the calcination process of the catalyst [11]. The EDX has revealed the composition of the catalyst, which further corroborated the XRD result in Figure 1.

Thermogravimetric analysis of the catalyst

The thermal response of trimetallic catalyst (Fe-Co-Mo) supported on $CaCO_3$ heated in an air environment was examined using thermogravimetric analysis (TGA). The result was represented in Figure 3. The weight loss as a function of the applied temperature was conducted to determine the feasibility of the catalyst in a CVD
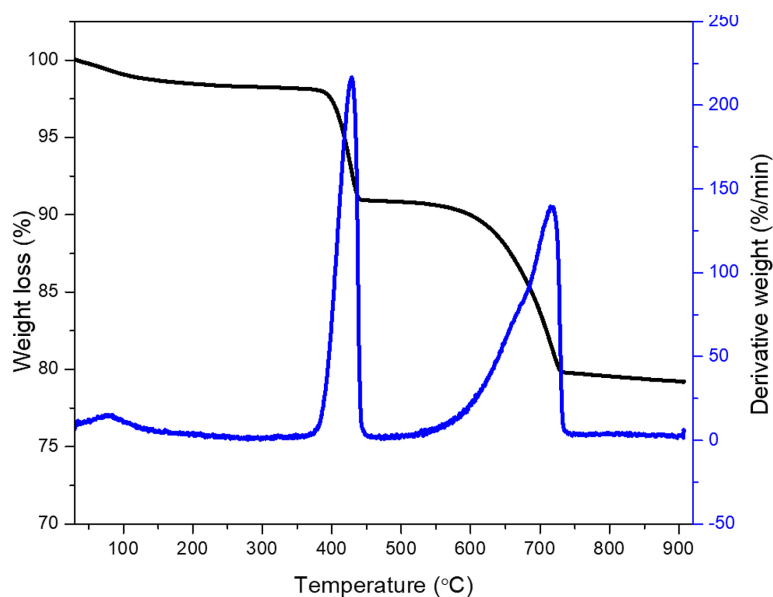

Fig. 3. TGA/DTG of prepared Fe-Co-Mo/CaCO₃ catalyst under air environment

reactor operated within the temperature range of 650–850 °C for CNTs synthesis. Figure 3 clearly shows two significant degradations that could be attributed to weight loss due to the loaded metal salts' transformation into the corresponding combination of metal oxides, such as $CoFe_2O_4$, $MoFe_2O_4$, and $MoCoFe_2O_4$. Weight loss also could result from the evolution of CO_2 when different mixed metallic oxides were formed when Fe, Co, and Mo salts interacted with $CaCO_3$ [11]. The first weight loss of ~7.1% started at ~380 °C with the peak of its first derivative at ~430 °C and could be attributed to metal salts changing to their corresponding metal oxides. The second weight loss of ~11.2% started at ~600 °C to 730 °C, which could be correlated to the putrefaction of $CaCO_3$ with the maximum decomposition rate at ~720 °C to form CaO and CO_2 [33]. The result demonstrated the catalyst's suitability for use in a CVD reactor for the synthesis of CNTs using the reaction temperature of 750 °C.

Characterization of the synthesized carbon nanotubes

XRD profile of the produced carbon nanotubes

Figure 4 shows XRD spectra of CNTs obtained from recycled PP and PE with the prepared catalyst of Fe-Co-Mo on $CaCO_3$ support. The existence of a robust diffraction peak of CNTs at 2θ of ~26.0° and 44.8° matched the plane (002) and (101) of the graphitized carbon in the CNTs

obtained from the waste plastics as carbon source [34], it is represented with the letter "C" in Figure 4 respectively. The peak intensity indicates the degree of crystallinity of the produced CNTs. It could be observed from Figure 4 that the intensity at 2θ of 26.0° for CNT obtained from PP was higher than that of PE. The crystalline carbon's d-spacing can be found using Bragg's equation ($d = \lambda/2 \sin\theta$) which were 0.3425 and 0.3442 nm for CNTs produced using waste PP and PE as carbon sources. These values are similar to the identical graphite d-spacing at 0.3354 nm, which suggests an excellent graphitic quality of the produced CNTs [12]. The other smaller peaks could be ascribed to catalyst impurities encapsulated in the CNTs [35].

Fourier transform infrared (FTIR)

FTIR study was performed to establish the surface functional groups available in the synthesized CNTs from recycled PP and PE as carbon sources. The spectra are shown in Figure 5, the spectra are identical with almost all the functional groups occurring at the same wave number. The broad peaks at 3436.54 cm^{-1} caused by the stretching vibrations of the hydroxyl (-OH) group indicates that water molecule was absorbed by the sidewalls of the CNTs [36], was observed in spectra of both CNTs obtained from PP and PE. The stretching bands of 2847.96 and 2854.77 cm^{-1} respectively were observed in both spectra which correspond to asymmetric and symmetric C-H of alkanes [37]. Most often, the existence of C-C and C-O bending
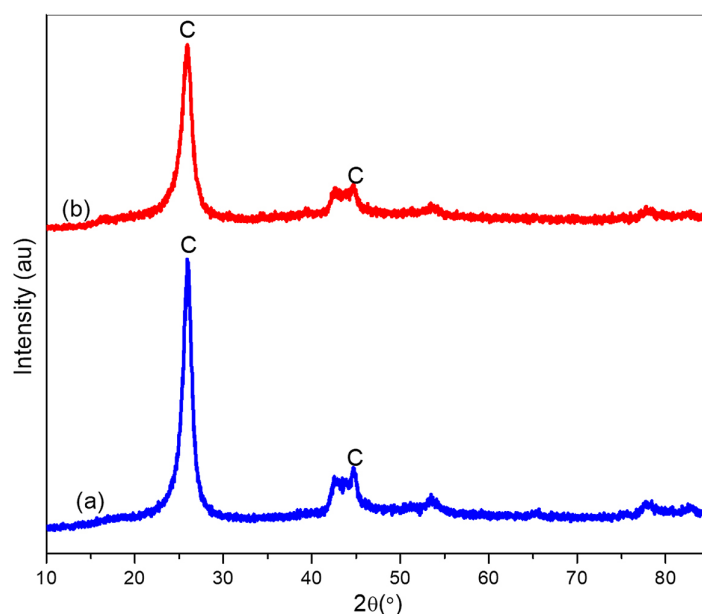

Fig. 4. XRD spectra of CNTs synthesized from recycled (a) PP and (b) PE as carbon sources over Fe-Co-Mo supported with $CaCO_3$ in a single CVD reactor system
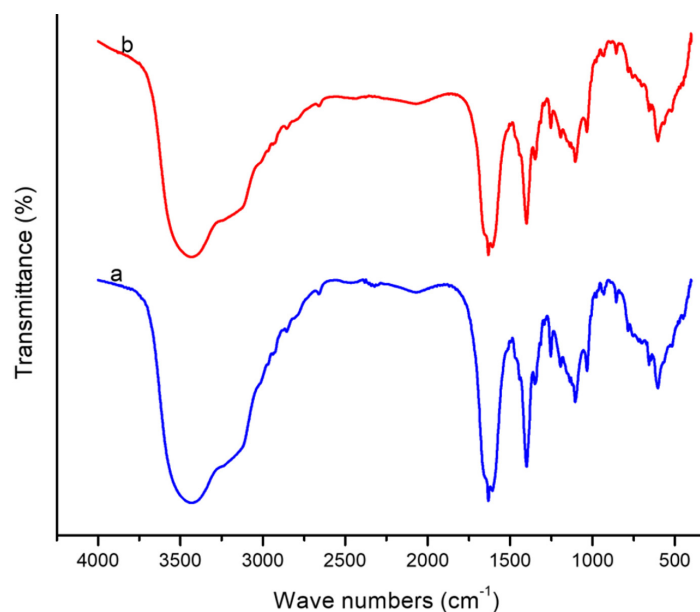
Fig. 5. FTIR spectrum of CNTs produced from recycled plastic wastes (a) PP and (b) PE over Fe-Co-Mo catalyst

bands between 600–1400 cm^{-1}, is mainly identi-fied as fingerprint zone [11]. These findings show that the surface of the produced CNTs was devoid of any major peaks connected to any unexpected functional groups in the produced CNTs.

Raman spectroscopy of the produced carbon nanotubes

The Raman spectra for the produced CNTs from waste PP and PE as feedstock over a trime-tallic catalyst of Fe-Co-Mo on CaCO$_3$ support in a CVD are presented in Figure 6. Raman spec-tra for CNTs produced from waste PP and PE

showed peaks at 1354 cm^{-1} for the D-band and 1582 and 1585 cm^{-1} for the G-band, respectively and 2D-band occurred at 2700 cm^{-1}. The peaks at 1582 and 1585 cm^{-1} corresponded to the G-band of graphite carbon, which relates to the vibration of sp^2-bonded carbon atoms in graphite sheets [36]. The D and G-bands suggested that amor-phous and ordered graphitic carbon are present in the synthesized samples. The 2D-band peak is observed in the products of the two samples, representing the resonance peak that could be related to the amount and purity of CNTs [38]. The intensity ratio of the D-band to the G-band
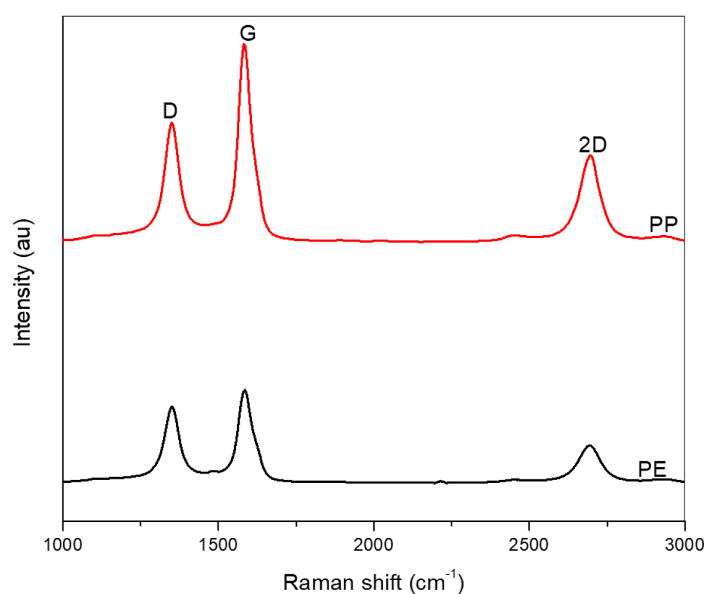

Fig. 6. Raman spectra of CNTs produced over a trimetallic catalyst of Fe-Co-Mo on CaCO$_3$ support using waste PP and PE as a carbon source in a single CVD reactor system

(I_D/I_G) describes the extent of graphitization of the deposited CNTs. The lower value of I_D/I_G indicates a higher quality, purity and structural ordering of CNTs [36]. The I_D/I_G ratio obtained for the synthesized CNTs were 0.6724 and 0.9028 using waste PP and PE, respectively. The results confirmed that the CNTs developed from PP were more graphitized compared to that of PE [12].

Comparison of yield and quality of CNTs produced from PP and PE

The summary of comparison of yield and quality of CNTs obtained from recycled PP and PE over the trimetallic catalyst of Fe-Co-Mo/CaCO$_3$ is presented in Table 1. Both feedstocks showed excellent potential for alternative carbon sources for CNTs synthesis as compared to the use of conventional hydrocarbon gases.

Surface area and pore size of synthesized CNTs

BET analysis of CNTs produced from recycled PP and PE as carbon sources was determined via N$_2$ physisorption at -196 °C detailed results were shown in Table 2. It could be observed that there are minimal differences in the properties of the CNTs produced from the PP and PE as carbon sources as it could be observed from the BET parameters. The surface area of CNT produced from PP waste was 6.834 m^2/g which is higher than the CNT produced from PE waste with surface area of 6.733 m^2/g. The slight differences observed in the BET and Langmuir surface areas could be attributed to impurities accumulated in the pores of the samples. The BET surface area graph analyses at -196 °C for the CNT samples are shown in Figure 7. From Figure 7 (a) it could be observed that the data from the CNT sample produced from PP gave a perfect linear with all the points fallen

Table 1. Product quality and yield of CNT from recycled polypropylene and polyethylene over Fe-Co-Mo/CaCO$_3$ catalyst

Carbon source	Polypropylene	Polyethylene
Amount of feed (g)	1.0	1.0
Catalyst (g)	0.1	0.1
Catalyst and carbon deposited (g)	0.4512	0.3376
Raman intensity ratio (I$_D$/I$_G$)	0.6724	0.9028
Yield (%)	35.12	23.76

Table 2. Parameters of BET analysis of as-synthesized CNTs from recycled PP and PE over Fe-Co-Mo/CaCO$_3$ catalyst

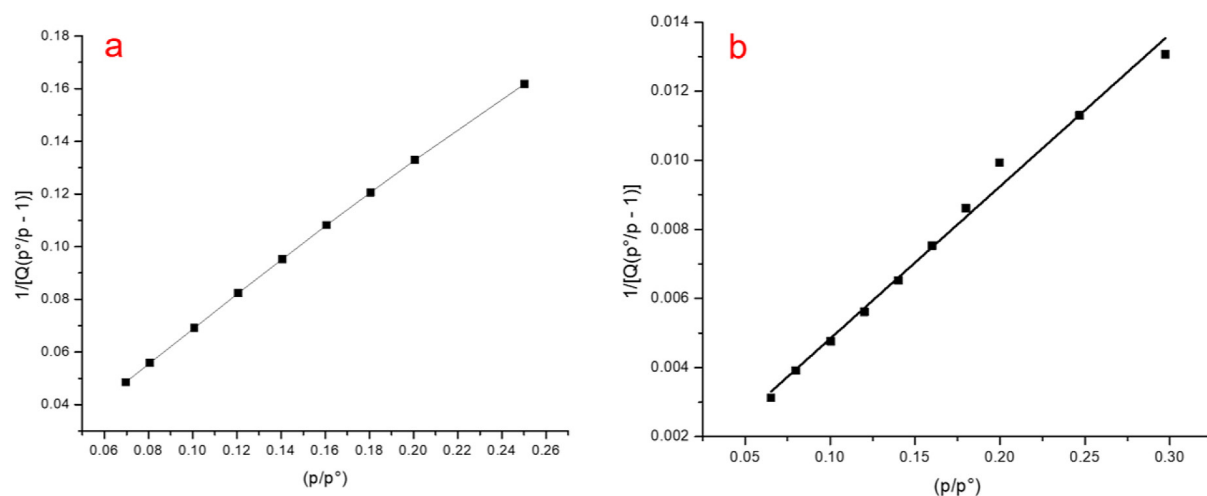| Carbon source	S$_{BET}$ Area (m^2/g)	Langmuir surface area (m^2/g)	Pore volume (cm^3/g)	Pore size (Å)
PP-CNT	6.834	70.468	0.0138	80.587
PE-CNT	6.733	70.347	0.0138	80.587

Fig. 7. BET-specific surface area plots of CNTs synthesized from recycled (a) PP and (b) PE over Fe-Co-Mo/CaCO$_3$ catalyst

on the line of the graph compared to the graph obtained for CNT produced from PE Figure 6 (b). This observation could be attributed to the extent of quality of the CNTs developed from PP and PE as carbon sources as corroborated by the Raman spectroscopy analysis depicted in Figure 6.

Thermogravimetric analysis (TGA) of the produced carbon nanotubes

The purity and quality of CNTs achieved from PP and PE over the catalysts Fe-Co-Mo/CaCO$_3$ were evaluated by thermal gravimetric analysis (TGA). The weight loss was attributed to the deposited carbon burnt in the air environment, which describes the yield of solid carbon on the catalysts [39]. Figures 8 (a) and (b) showed the percentage weight loss of CNTs produced from waste PP and PE, signifying that the samples have high carbon content, which described high purity CNTs corresponding to 94.71% and 94.40%. The contaminants in the CNT samples may have been caused by leftover catalysts from the process and other species that may have been present in the samples. An acid leaching has been used to treat the CNT samples to separate the residual catalyst particles from other substances, such as residual catalysts. Amorphous carbon has many more structural defects than graphitic carbon and burns at a lower temperature of around 400 °C [40], while graphitic carbon burns between 600 to 700 °C [41]. The DTG profiles showed mono peak for each product at 650.60 and 648.30 °C for CNTs produced using PP and PE as carbon feedstock, respectively, which could be attributed to oxidation of CNT of larger diameter coated with a layer of carbon [42].

Transmission electron microscopy (TEM)

TEM was employed to study the morphological characteristics of the CNTs with more precision and accuracy. TEM images of the deposited CNTs were collected, and the results demonstrated that CNT wall structures differ, and their diameter distribution is not uniform, as shown in Figure 9. Metal catalyst nanoparticles are encapsulated inside CNTs as they develop through a tip or root mechanism. The diameter of the final nanotubes may vary depending on how small the metal particles are [43]. Hence, the wide-diameter distributions of CNTs are caused by the varied metal sizes in the catalyst alloy. As a result of the diverse sizes of the catalyst metal nanoparticles, the CNTs outer diameters and wall structures vary. The average diameter of the synthesized CNTs from PP and PE were 36 and 34 nm respectively. It is obvious from the TEM images that CNTs produced from PP and PE showed a long hollow core MWCNTs. Similar results were reported by [27]. Additionally, the nanotube's interior and exterior surfaces seem to be quite even and smooth. These findings proved that the catalyst created MWCNTs in the graphene layers that were of good quality and with few flaws. However, the agglomeration of certain catalyst metallic particles that were not in contact with one another during the reduction process may be responsible for the occurrence of relatively large-diameter MWCNTs. The SAED of the synthesized CNTs was shown together with the TEM in Figure 9. It exhibits a circle diffraction pattern of the MWCNTs. The interplanar spacing of the CNTs crystal structure was used to name the ring pattern
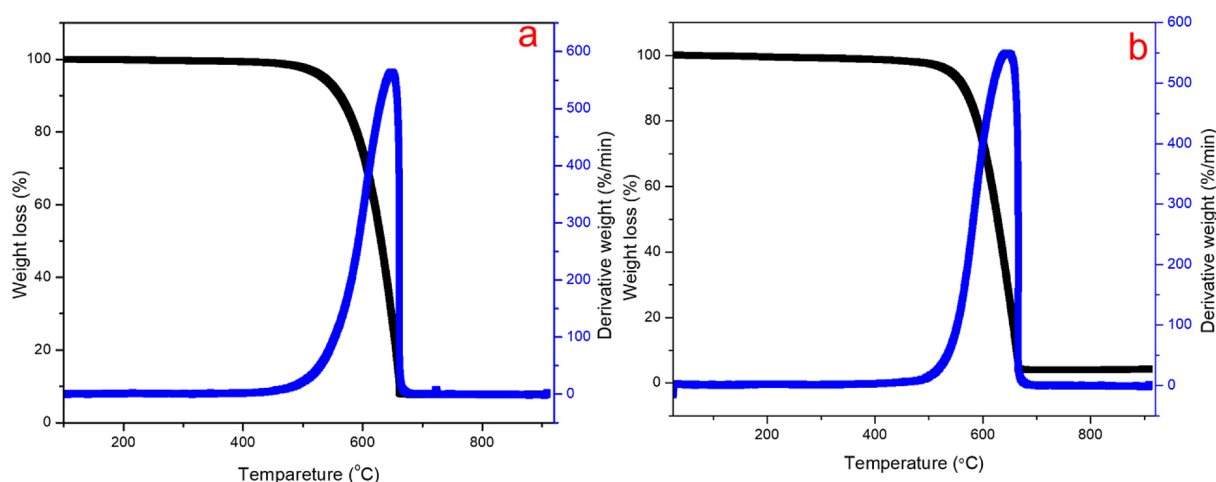

Fig. 8. TG/DTG profiles of as-synthesized CNTs from PP (a) and PE (b) as carbon sources over Fe-Co-Mo on calcium carbonate support
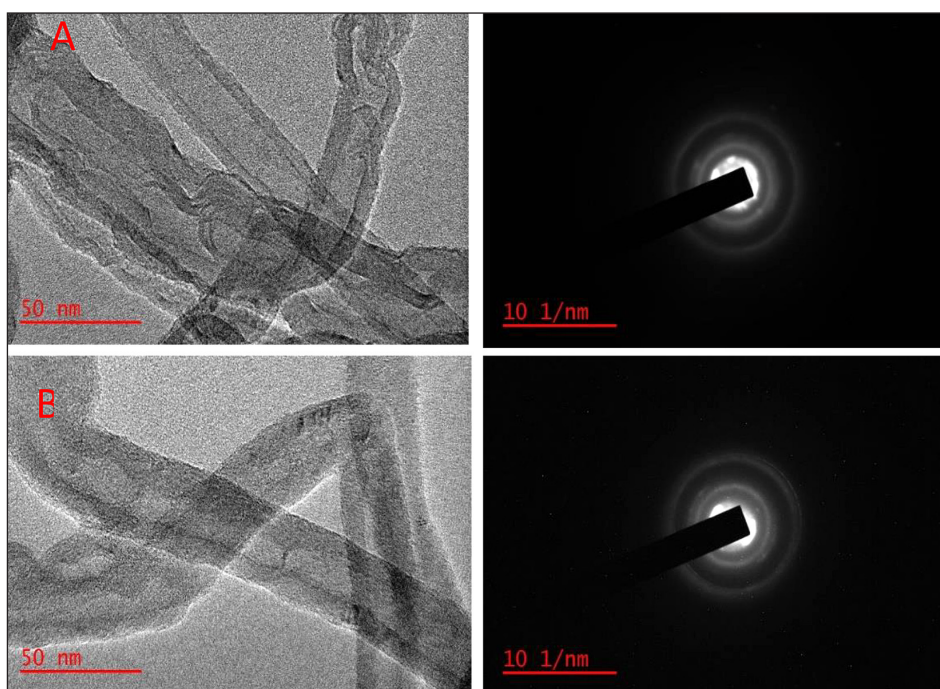
Fig. 9. TEM and SEAD of CNTs obtained from PP (A) and PE (B) over Fe-Co-Mo/CaCO$_3$ catalyst respectively

using the Miller indices [44]. A sample's ring pattern shows a crystal structure similar to the ring pattern found in graphite. Therefore, MWCNTs' interplanar spacing is essentially identical to that of graphite. The graphite crystal structure was used to measure the interplanar spacing of CNTs.

CONCLUSIONS

The prospect of developing high-value products from PW stream, often viewed as a problem, has become attractive due to the growing perception of waste plastics as a resource. The benefits derived from CNTs and potential revenues generated from them have fascinated the conversion of PW into CNTs through different approaches. This study successfully used the CVD technique to synthesize MWCNTs from PP and PE wastes over Fe-Co-Mo catalyst supported on calcium carbonate. The XRD, Raman, and TGA confirmed high graphitic carbon in the synthesized products. The d-spacing of CNTs from XRD analysis was 0.3425 nm and 0.3442 nm for products obtained from PP and PE as feedstocks, respectively. The BET and Langmuir surface areas were found to be (6.834 and 70.468 m^2/g) and (6.733 and 70.347 m^2/g) for CNTs obtained from PP and PE respectively. The Raman analysis established the degree of graphitization and the computed I_D/I_G to be 0.6724 and 0.9028 for CNTs obtained

from PP and PE, respectively. The TEM images clearly showed the formation of MWCNT. Although recycled PP showed a higher percentage yield and quality over PE; nonetheless, the two materials have been shown to provide alternative feedstocks for CNT synthesis using the CVD technique. CNTs produced in this study could be used in diverse spheres of scientific applications such as energy storage, adsorbent for emerging pollutants removal from wastewater, ultra-strong light-weight materials development, biomedical, smart nanomaterial development and so on.

Declaration of competing interest

The authors declared no financial or interpersonal conflicts of interest.

Acknowledgment

REFERENCES

1. W.U. Eze, R. Umunakwe, H.C. Obasi, M.I. Ugbaja, C.C. Uche, and I.C. Madufor, Plastics waste management: A review of pyrolysis technology, Clean Technologies and Recycling, vol. 1, pp. 50–69,

2021. doi: 10.3934/ctr.2021003.

2. N. Evode, S.A. Qamar, M. Bilal, D. Barceló, and H.M.N. Iqbal, Plastic waste and its management strategies for environmental sustainability. Case Studies in Chemical and Environmental Engineering, vol. 4, p. 100142, 2021. doi: https://doi.org/10.1016/j.cscee.2021.100142

3. K. Li, H. Zhang, Y. Zheng, G. Yuan, Q. Jia, and S. Zhang, Catalytic Preparation of Carbon Nanotubes from Waste Polyethylene Using FeNi Bimetallic Nanocatalyst. Nanomaterials, vol. 10, no. 8, p. 1517, 2020. doi: https://doi.org/10.3390/nano10081517

4. D. Kawecki, P.R.W. Scheeder, and B. Nowack, Probabilistic material flow analysis of seven commodity plastics in Europe. Environmental science & technology, vol. 52, no. 17, pp. 9874–9888, 2018. doi: https://doi.org/10.1021/acs.est.8b01513

5. O.O. Ayeleru et al., Challenges of plastic waste generation and management in sub-Saharan Africa: A review. Waste Management, vol. 110, pp. 24–42, 2020. doi: https://doi.org/10.1016/j.wasman.2020.04.017

6. D. Yao, Y. Zhang, P. T. Williams, H. Yang, and H. Chen, Co-production of hydrogen and carbon nanotubes from real-world waste plastics: Influence of catalyst composition and operational parameters. Applied Catalysis B: Environmental, vol. 221, pp. 584–597, 2018. doi: https://doi.org/10.1016/j.apcatb.2017.09.035.

7. A.A.Aboul-Enein, H. Adel-Rahman, A.M. Haggar, and A.E. Awadallah, Simple method for synthesis of carbon nanotubes over Ni-Mo/Al2O3 catalyst via pyrolysis of polyethylene waste using a two-stage process. Fullerenes, Nanotubes and Carbon Nanostructures, vol. 25, no. 4, pp. 211–222, 2017. doi: http://dx.doi.org/10.1080/1536383X.2016.1277422.

8. G. Litak, Buckling behaviour of single-walled carbon nanotubes under axial loading. Advances in Science and Technology. Research Journal, vol. 11, no. 1, pp. 208–211, 2017. doi: 10.12913/22998624/68468.

9. M. Arda and M. Aydogdu, Analysis of free torsional vibration in carbon nanotubes embedded in a viscoelastic medium. Advances in Science and Technology. Research Journal, vol. 9, no. 26, pp. 28–33, 2015. doi: 10.12913/22998624/2361.

10. H.U. Modekwe, M.A. Mamo, M.O. Daramola, and K. Moothi, Catalytic Performance of Calcium Titanate for Catalytic Decomposition of Waste Polypropylene to Carbon Nanotubes in a Single-Stage CVD Reactor. Catalysts, vol. 10, no. 9, p. 1030, 2020. doi: https://www.mdpi.com/2073-4344/10/9/1030#.

11. A.S. Abdulkareem, I. Kariim, M.T. Bankole, J.O. Tijani, T. Abodunrin, and S. Olu, Synthesis and Characterization of Tri-metallic Fe-Co-Ni Catalyst Supported on CaCO$_3$ for Multi-Walled Carbon Nanotubes Growth via Chemical Vapor Deposition Technique.

Arabian Journal for Science & Engineering (Springer Science & Business Media BV), vol. 42, no. 10, 2017. doi: 10.1007/s13369-017-2478-2.

12. A.A. Ezz, M.M. Kamel, and G.R. Saad, Synthesis and characterization of nanocarbon having different morphological structures by chemical vapor deposition over Fe-Ni-Co-Mo/MgO catalyst. Journal of Saudi Chemical Society, vol. 23, no. 6, pp. 666–677, 2019. doi: https://doi.org/10.1016/j.jscs.2018.11.004.

13. K.J. Kim et al., The effect of carbon nanotube diameter on the electrical, thermal, and mechanical properties of polymer composites. Carbon letters, vol. 26, pp. 95–101, 2018. doi: 10.5714/CL.2018.26.095.

14. B. Arora and P. Attri, Carbon nanotubes (CNTs): a potential nanomaterial for water purification. Journal of Composites Science, vol. 4, no. 3, p. 20, 2020. doi: 10.3390/jcs4030135.

15. S. He, Y. Xu, Y. Zhang, S. Bell, and C. Wu, Waste plastics recycling for producing high-value carbon nanotubes: Investigation of the influence of Manganese content in Fe-based catalysts. Journal of Hazardous Materials, vol. 402, p. 123726, 2021. doi: https://doi.org/10.1016/j.jhazmat.2020.123726.

16. X. Liu, S. He, Z. Han, and C. Wu, Investigation of spherical alumina supported catalyst for carbon nanotubes production from waste polyethylene. Process Safety and Environmental Protection, vol. 146, pp. 201–207, 2021. doi: https://doi.org/10.1016/j.psep.2020.08.027.

17. P. . Tripathi, S. Durbach, and N.J. Coville, Synthesis of multi-walled carbon nanotubes from plastic waste using a stainless-steel CVD reactor as catalyst. Nanomaterials, vol. 7, no. 10, p. 284, 201. doi: 10.3390/nano7100284.

18. K. Shah et al., Conversion of pyrolytic non-condensable gases from polypropylene co-polymer into bamboo-type carbon nanotubes and high-quality oil using biochar as catalyst. Journal of Environmental Management, vol. 301, p. 113791, 2022. doi: https://doi.org/10.1016/j.jenvman.2021.113791.

19. N. Kure et al., Simple microwave-assisted synthesis of carbon nanotubes using polyethylene as carbon precursor. Journal of Nanomaterials, vol. 2017, 2017. doi: https://doi.org/10.1155/2017/2474267.

20. J. Song, H. Zhang, J. Wang, L. Huang, and S. Zhang, High-yield production of large aspect ratio carbon nanotubes via catalytic pyrolysis of cheap coal tar pitch. Carbon, vol. 130, pp. 701–713, 2018. doi: https://doi.org/10.1016/j.carbon.2018.01.060.

21. N. Miskolczi, J. Sója, and E. Tulok, Thermo-catalytic two-step pyrolysis of real waste plastics from end of life vehicle. Journal of Analytical and Applied Pyrolysis, vol. 128, pp. 1–12, 2017. doi: https://doi.org/10.1016/j.jaap.2017.11.008.

22. R. Shoukat and M. I. Khan, Carbon nanotubes: A review on properties, synthesis methods and applications in micro and nanotechnology. Microsystem Technologies, vol. 27, no. 12, pp. 4183–4192, 2021. doi: https://doi.org/10.1007/s00542-021-05211-6.

23. H.U. Modekwe, M.A. Mamo, K. Moothi, and M.O. Daramola, Synthesis of bimetallic NiMo/MgO catalyst for catalytic conversion of waste plastics (polypropylene) to carbon nanotubes (CNTs) via chemical vapour deposition method. Materials Today: Proceedings, vol. 38, pp. 549–552, 2021. doi: https://doi.org/10.1016/j.matpr.2020.02.398.

24. L.M. Esteves, J.L. Smarzaro, A. Caytuero, H.A. Oliveira, and F.B. Passos, Catalyst preparation methods to reduce contaminants in a high-yield purification process of multiwalled carbon nanotubes. Brazilian Journal of Chemical Engineering, vol. 36, pp. 1587–1600, 2020. doi: dx.doi.org/10.1590/0104-6632.20190364s2019025.

25. P. Setyopratomo, P.P.D.K. Wulan, and M. Sudibandriyo, Carbon nanotubes synthesis using Fe-Co-Mo/MgO tri-metallic catalyst: study the effect of reaction temperature, reaction time and catalyst weigh. International Journal of Nanomanufacturing, vol. 16, no. 1, pp. 1–20, 2020. doi: https://dx.doi.org/10.1504/IJNM.2020.104476.

26. A.A. Aboul-Enein and A.E. Awadallah, Impact of Co/Mo ratio on the activity of CoMo/MgO catalyst for production of high-quality multi-walled carbon nanotubes from polyethylene waste. Materials Chemistry and Physics, vol. 238, p. 121879, 2019. doi: https://doi.org/10.1016/j.matchemphys.2019.121879.

27. A.A.Aboul-Enein and A.E. Awadallah, Production of nanostructure carbon materials via non-oxidative thermal degradation of real polypropylene waste plastic using La_2O_3 supported Ni and Ni–Cu catalysts. Polymer Degradation and Stability, vol. 167, pp. 157–169, 2019. doi: https://doi.org/10.1016/j.polymdegradstab.2019.06.015.

28. S.M. Abdelbasir, K.M. McCourt, C.M. Lee, and D.C. Vanegas, Waste-derived nanoparticles: synthesis approaches, environmental applications, and sustainability considerations. Frontiers in Chemistry, vol. 8, p. 782, 2020. doi: https://doi.org/10.3389/fchem.2020.00782.

29. J. Wang, B. Shen, M. Lan, D. Kang, and C. Wu, Carbon nanotubes (CNTs) production from catalytic pyrolysis of waste plastics: The influence of catalyst and reaction pressure. Catalysis Today, vol. 351, pp. 50–57, 2020. doi: https://doi.org/10.1016/j.cattod.2019.01.058.

30. S.U. Rather, Trimetallic catalyst synthesized multi-walled carbon nanotubes and their application for hydrogen storage. Korean Journal of Chemical Engineering, vol. 33, no. 5, pp. 1551–1556, 2016. doi: https://link.springer.com/article/10.1007/s11814-015-0271-z.

31. D. Yao, H. Yang, Q. Hu, Y. Chen, H. Chen, and P.T. Williams, Carbon nanotubes from post-consumer waste plastics: Investigations into catalyst metal and support material characteristics. Applied Catalysis B: Environmental, vol. 280, p. 119413, 2021. doi: https://doi.org/10.1016/j.apcatb.2020.119413.

32. A. Karbul, M.K. Mohammadi, R.J. Yengejeh, and F. Farrokhian, Synthesis and Characterization of Trimetallic Fe-Co-V/Zeolite and Fe-Co-Mo/Zeolite Composite Nanostructures. Materials Research, vol. 24, no. 3, p. 7, 2021. doi: https://doi.org/10.1590/1980-5373-MR-2020-0292.

33. K.S.P. Karunadasa, C.H. Manoratne, H.M.T.G.A. Pitawala, and R.M.G. Rajapakse, Thermal decomposition of calcium carbonate (calcite polymorph) as examined by in-situ high-temperature X-ray powder diffraction. Journal of Physics and Chemistry of solids, vol. 134, pp. 21–28. 2019, doi: https://doi.org/10.1016/j.jpcs.2019.05.023.

34. A. Aliyu, A.S. Abdulkareem, A.S. Kovo, O.K. Abubakre, J.O. Tijani, and I. Kariim, Synthesize multi-walled carbon nanotubes via catalytic chemical vapour deposition method on Fe-Ni bimetallic catalyst supported on kaolin. Carbon Letters vol. 21, pp. 33–50, 2017. doi: https://doi.org/10.5714/CL.2017.21.033.

35. F.H. Abdulrazzak, A.F. Alkiam, and F.H. Hussein, Behavior of X-ray analysis of carbon nanotubes. in Perspective of carbon nanotubes: IntechOpen London, UK, 2019.

36. H.U. Modekwe, K. Moothi, M.O. Daramola, and M.A. Mamo, Corn Cob Char as Catalyst Support for Developing Carbon Nanotubes from Waste Polypropylene Plastics: Comparison of Activation Techniques. Polymers, vol. 14, no. 14, p. 2898, 2022. doi: https://www.mdpi.com/2073-4360/14/14/2898#.

37. Z. Zhao, Z. Yang, Y. Hu, J. Li, and X. Fan, Multiple functionalization of multi-walled carbon nanotubes with carboxyl and amino groups. Applied surface science, vol. 276, pp. 476–481, 2013. doi: https://doi.org/10.1016/j.apsusc.2013.03.119.

38. E.D. Dikio, N.D. Shooto, F.T. Thema, and A.M. Farah, Raman and TGA study of carbon nanotubes synthesized over Mo/Fe catalyst on aluminium oxide, calcium carbonate and magnesium oxide support. Chemical Science Transactions, vol. 2, no. 4, pp. 1160–1173, 2013. doi: 10.7598/cst2013.519.

39. S. Saconsint et al., Development of high-performance nickel-based catalysts for production of hydrogen and carbon nanotubes from biogas. Scientific Reports, vol. 12, no. 1, p. 15195, 2022. doi: 10.21203/rs.3.rs-1839692/v1.

40. A. Buzarovska, V. Stefov, M. Najdoski, and G. Bogoeva-Gaceva, Thermal analysis of multi-walled carbon nanotubes material obtained by catalytic

pyrolysis of polyethylene. Macedonian Journal of Chemistry and Chemical Engineering, vol. 34, no. 2, pp. 373–379, 2015. doi: 10.20450/mjcce.2015.620.

41. A. Mahajan, A. Kingon, A. Kukovecz, Z. Konya, and P.M. Vilarinho, Studies on the thermal decomposition of multiwall carbon nanotubes under different atmospheres. Materials Letters, vol. 90, pp. 165-168, 2013. doi: https://doi.org/10.1016/j.matlet.2012.08.120.

42. Y. Liu et al., Synthesis of porous carbon nanotubes foam composites with a high accessible surface area and tunable porosity. Journal of Materials Chemistry A, vol. 1, no. 33, pp. 9508–9516, 2013. doi: http://dx.doi.org/10.1039/C3TA10695K.

43. I.A. Mohammed, M.T. Bankole, A.S. Abdulkareem, S.S. Ochigbo, A.S. Afolabi, and O.K. Abubakre, Full factorial design approach to carbon nanotubes synthesis by CVD method in argon environment. South African Journal of Chemical Engineering, vol. 24, no. 1, pp. 17–42, 2017. doi: https://doi.org/10.1016/j.sajce.2017.06.001.

44. M.J. Eskandari, M.A. Asadabad, R. Tafrishi, and M. Emamalizadeh, Transmission electron microscopy characterization of different nanotubes. Inorganic and nano-metal chemistry, vol. 47, no. 2, pp. 197–201, 2017. doi: https://doi.org/10.1080/15533174.2015.1137317.